Military Technical College
Kobry El-Kobbah,
Cairo, Egypt.

17th International Conference on Applied Mechanics and Mechanical Engineering.

EFFECT OF JATROPHA BIOFUEL VISCOSITY ON INTERNAL TWO PHASE FLOW INSIDE FFERVESCENT ATOMIZER FOR GAS TURBINE APPLICATIONS

A. Helmy*, S.A.Wilson** and A. Balabel**

ABSTRACT

In the current work, three-dimensional simulations of the internal flow inside effervescent atomizer are performed. For this purpose, the volume of fluid model combined with the two equation realizable k-ε turbulence model are adopted. Validation with previous work in the literature is performed and the current results compare well. The internal flow results are then compared for both jet-A1 fuel and jatropha biofuel, as alternative fuel for commercial aviation. The present results show that the flow inside the atomizer evolves with gas to liquid mass ratio (GLR). Slug flow is identified for both fuels at low GLRS (below 0.3%) while annular flow is obtained at higher GLRs (above 0.3%). The effect of biofuel viscosity on the flow is obvious at GLRs below 0.3% and is relatively inhibited at higher values of GLR (0.8%). Finally the current results show the capability of effervescent atomizer in handling jatropha biofuel, in terms of internal flow.

KEY WORDS

Jatropha biofuel, effervescent atomizer, two-phase flow, volume of fluid and aviation

* Assist. Lecturer, Dept. of Mech. Power Eng., Menofia Univ., Shebin El-Kom, Egypt.
** Professor, Dept. of Mech. Power Eng., Menofia University, Shebin El-Kom, Egypt.

NOMENCLATURE

D	Diameter
f	Interfacial force
g	Acceleration due to gravity
h	Liquid film thickness
P	pressure
R	Radius
S	Interaction source term
u	Velocity component
α	Volume fraction
δ	Surface tension coefficient
ε	Turbulent energy dissipation
ϕ	General flow variable
k	Turbulent kinetic energy
κ	Surface curvature
μ	Molecular viscosity
ρ	Density
τ	Reynolds stress tensor

INTRODUCTION

In the last decades, Commercial aviation has considered as one of the most used transportation and has grown from novelty to essential. Today, most of commercial aviation systems use the gas turbine engines as a power source, due to the extreme specific power requirement. Unfortunately, most of these engines depend on the combustion of jet-A1 fossil fuels [1], which is accompanied with energy crisis issues and bad environmental effects [2]. So replacement of jet-A1 fossil fuel is vital to insure steady fuel supply and to reduce carbon-footprint of aviation.

One of the promising alternatives is Jatropha biofuel [3]. This is due to sustainability, ability to be cultivated in deserts with only rain or even treated sewage water in addition to inedibility [3]. Technically, several airlines have experimented safely using of jatropha biofuels blended with jet-A1 fuel (50-50 %) on commercial flights [4-6]. Airbus reported that jatropha has the potential to reduce the overall CO_2 footprint by up to 80 percent over standard aviation kerosene [6]. Boeing stated that, jatropha can deliver strong environmental and socioeconomic benefits and greenhouse gas reductions of up to 60 percent when compared with petroleum based jet fuel [6]. But, all of these trials have employed blends which is still dependent on jet-A1 fossil fuel that finally will be extinct. So, using pure jatropha biofuel in commercial aviation will be the final destination towards totally replacing the fossil fuel. But introducing pure jatropha biofuel to gas turbine engine encounters several challenges, due to the high viscosity and surface tension relevant with biofuel as can depicted from table.1. This leads to bad atomization characteristics in terms of larger droplets size and low mixing rates, which inhibit complete combustion inside the engine [7]. Therefore, the target now is to enhance the jatropha biofuel atomization. In the literature and from the various atomization techniques, effervescent atomization [8-10] is one of the promising atomization techniques dedicated for high viscosity fuels. This atomization method is internal mixing twin fluid technique. It has been shown to produce well-atomized spray

with only small amount of atomizing gas at low injection pressure [8, 9]. Further, it has the capability of atomizing high viscosity fuels well [10].

The basic idea of effervescent atomizer was first sparked in the late of 1980's by Lefebvre [8]. A new atomization technique was developed by loading the bulk liquid with bubbles of the atomizing gas upstream of the final discharge orifice of the atomizer. The gas was injected inside the liquid by means of aerating tube. The gas bubbles suspended in the liquid form two-phase bubbly mixture. Like the trapped air bubbles in an opened water tap, the bubbles explode just at atomizer exit, which enhance shattering the liquid fuel into finer droplets. Further, the presence of gas bubbles inside the atomizer squeezes the liquid as the gas occupies large portion due to its higher specific volume. The reduced liquid characteristic length at atomizer exit enhances the liquid atomization in turn [8, 9]. Moreover, the squeezed liquid becomes faster, to preserve flow continuity, which enhance liquid shattering and shear [8]. However, by this technique it is only needed from the atomizing gas to occupy some volumes inside the liquid fuel in the form of bubbles. So the gas is not required to possess high kinetic energy as in the case of other twin fluid atomizers [11].

The internal flow inside effervescent atomizer is one of the most contributory factors affecting the atomizer performance and corresponding produced spray to great extent [11], as the atomizer is internal mixing twin fluid atomizer. However, most of the studies in literature have been focused on the external flow and relatively fewer studies were directed to the internal two-phase flow inside the atomizer [11]. This may be attributed to the difficulties associated with flow in micro channels and the relevant complex physical phenomena. Lin et al. [12] used flow visualization to investigate the two-phase flow corresponding to transparent effervescent atomizers. Various aerating tube configuration, several converging angle connecting mixing chamber and discharge passage and the effect of gas to liquid mass ratio (GLR) were tested. They concluded that the internal flow structures have a great influence on the corresponding produced spray. The results showed the transition in internal flow structures from bubbly flow in the mixing chamber to slug flow in the final passage, to a co-annular flow as the aeration level increases. They also observed that the co-annular flow regime dominates at high aeration level. They noticed steady spray with co-annular regime inside the atomizer. Further, a correlation relating liquid film thickness in discharge passage with gas to liquid mass ratio (GLR) was fitted. In agreement with the observations done by Lin et al. [12] and Jobehdar et al. [13], Locher et al. [14] distinguished between main flow regimes in the discharge passage, bubbly, slug and annular flow with increasing aeration levels, by measuring the void fraction. Further, they noticed that gas bubbles elongate and expand in the discharge passage due to the increase in velocity [9,14,15].

In view of the difficulties accompanying experimental work on two-phase flow, numerical simulations were performed to investigate two-phase flow evolution inside effervescent atomizer. Law et al. [15] simulated the dynamic shapes and sizes of single air bubbles injected in liquid water cross flow of an effervescent atomizer's mixing chamber. They used the volume of fluid module in ANSYS-FLUENT commercial code. They found that bubbles within the convergent section deformed into a conical shape. Further, velocity fluctuations at the atomizer exit were found to exist for both the liquid and air as the bubble traverses and exits the nozzle. They considered these velocity

fluctuations at the nozzle exit as possible means for disrupting and enhancing liquid break-up as compared to simple pressure atomization of the liquid phase alone [15].

Esfarjani and Dolatabadi [16] used the Eulerian-Eulerian two-fluid model to simulate the three-dimensional structure of two-phase laminar flow inside the effervescent atomizer of the experimental of Lin et al. [12]. It was observed that the liquid film thickness in the discharge passage is slightly independent of liquid physical properties such as viscosity. The flow evolved from slug flow to annular flow with increasing GLRs. They recommended that the turbulence effects must be considered in future simulations.

Mehmood and Masud [17] simulated the internal flow inside the effervescent atomizer used by Esfarjani and Dolatabadi [16]. They used of the Volume of fluid (VOF) technique using ANSYS FLUENT. The flow structure was observed at various GLRs, ranging from 0.08 % to 1.25 %. It was observed that at low GLR of 0.08% the gas phase in the mixing chamber can be identified as relatively large bubbles flowing in the liquid phase. The large bubbles evolve into large slugs of gas while entering the discharge passage. At higher GLR of 1.25%, the annular flow dominates.

To the best of our knowledge, no experimental or numerical studies in the literature were addressed to investigate the internal flow inside effervescent atomizer with biofuel application. So, the present study aims to numerically investigate the applicability of effervescent atomizer to handle jatropha biofuel as alternative fuel for commercial aviation. In the current study, the configuration used in the Air Force Research Laboratory (AFRL) [12] was modeled to numerically investigate the structures of the internal flow inside effervescent atomizer with Jatropha biofuel. Further, flow evolution and the liquid film thickness in the discharge passage were investigated. Finally, the results of jatropha biofuel were compared with conventional commercial aviation jet A-1 fuel.

MATHEMATICAL MODELLING

Model Selection

In the literature, two distinct techniques were used to simulate to internal two-phase flow (gas/liquid) inside effervescent atomizer; Eulerian-Eulerian model [16] and interface tracking volume of fluid model [15, 17]. In Eulerian-Eulerian modelling the gas bubbles diameters are a prerequisite [16, 18], which are not available for new simulations as the case in the current study. Consequently, the volume of fluid model is adopted in the present work. The volume of fluid model, sometimes called one fluid model, treats the two phases as single fluid, in a fixed Eulerian frame work, with variable properties corresponding to the dominant phase in each zone. For zones where both the two phases exist, mixing properties according to the weight of each phase are calculated. So only one set of governing equations is needed. In addition, a supplementary equation represent volume of the liquid is solved [16]. A reconstruction of the interface between the two phases is then performed using different algorithms to define the interface between the two phases accurately according to the gradient of calculated volume of fluid [19].

Governing Equations

The flow inside the atomizer is considered incompressible isothermal flow, so only the continuity and momentum equations are applied. For turbulence modelling, the two equation realizable k-ε model [20] is selected, according to the work of Mehmood and Masud [17]. In addition, the volume of fluid equation incorporated in the VOF model is solved [19]. The equations of continuity, momentum and volume of fluid, in compact form, can be written as;

$$\frac{\partial \rho u_j}{\partial x_j} = 0 \tag{1}$$

$$\frac{\partial \rho u_i u_j}{\partial x_j} = -\frac{\partial p}{\partial x_i} + \frac{\partial \tau_{ij}}{\partial x_j} + S_{mon} \tag{2}$$

$$\frac{\partial \rho \alpha}{\partial x_j} = 0 \tag{3}$$

where, $S_{mon} = \rho\, \mathrm{g}_i + \mathrm{f}_\delta$ is the momentum source term due to both gravity $\rho\, \mathrm{g}_i$, and surface tension forces f_δ, and α is liquid phase volume fraction. τ_{ij} is the Reynolds stress tensor of eddy viscosity model that is given by,

$$\tau_{ij} = \mu_e \left(\frac{\partial u_i}{\partial x_j} + \frac{\partial u_j}{\partial x_i}\right) \tag{4}$$

where, $\mu_e = \mu + \mu_t$ is the effective turbulent viscosity and μ_t is the turbulent viscosity, calculated from the adopted turbulence model. The equation of turbulent kinetic energy (k) and turbulent dissipation rate (ε) are described, in more details, in ANSYS FLUENT-15 module [20].

Surface Tension Modelling

Without surface tension, no bubble would be curved. Surface tension controls the bubbles diameters in gas-liquid flows. Therefore, modelling surface tension is necessary for accurate interface tracking. For this purpose, the continuum surface force model of Brackbill et al. [21] is used. In this model, the surface tension force tends to increase the pressure of the gas at the interface. A balance between pressure drop across the surface and surface tension force is performed, considering only the normal forces. The surface tension is calculated by getting the curvature of the interface at two radii; R_1 and R_2, then the following equation can be deduced;

$$P_2 - P_1 = \delta \left(\frac{1}{R_1} + \frac{1}{R_2}\right) \tag{5}$$

where $P_2 - P_1$is the pressure jump across the interface due to surface tension and δ is the surface tension coefficient. After managements [20, 21], the source term incorporated in the momentum equation due to surface tension (f_δ) can be written as;

$$f_\delta = \delta \frac{\rho \kappa_i \nabla \alpha_i}{0.5(\rho_i + \rho_j)} \quad (6)$$

where i, j refer to the phases, ρ is the mixture density and κ is the curvature at the interface, it can be deduced from the gradient of α in the normal direction to the interface.

GEOMETRY

The VI configuration used by Lin et al. [12] is selected for the current simulation, following the work of Esfarjani and Dolatabadi [16] and Mehmood and Masud [17]. The proposed atomizer has a rectangular cross section with thickness is 2 mm. the atomizer geometry and dimension are shown in Fig.1. Further, in the current study and in contrast to the previous simulations conducted in the same atomizer, the simulated atomizer geometry was extended to include the inlet section for both phases. Therefore, 20 mm inlet section was modelled in addition to the mixing chamber and discharge passage. The thickness of the aerating duct is 350 μm. This enables to account for the relevant physical phenomena such as vortex shedding at mixing chamber inlet, which with no doubt affects flow nature.

COMPUTATIONAL DOMAIN AND BOUNDARY CONDITIONS

Three-dimensional simulation is important for accurate simulations. However, to reduce computational effort, geometry symmetry around z-axis in x-y plane is considered and only on half of the domain is simulated [16], as shown in Fig.1. Structured quad mesh is adopted in grid generation process. To do so, domain decomposition is performed and the geometry was decomposed to 24 grid blocks. The total number of mesh is around 0.6 million cell. Further, the cells were clustered near the wall to capture the near-wall region. The boundary conditions used are also shown in Fig. 2. For inlet, velocity inlet boundary condition is applied for the two phases. The inlet velocity is calculated from the mass flow rate of each phase and the corresponding inlet cross section area. The inlet turbulence-parameters are calculated from the turbulence intensity, which is calculated according to the Reynolds number (Re) [20], as indicated in equation (7). The volume fraction at inlet is given either 1 or 0 according to the dominant phase. For outlet, pressure outlet boundary condition with exit pressure of 1 atm is used. No slip stationary wall boundary condition is applied at all atomizer walls. Symmetry boundary condition is applied at symmetry plane around z-axis as indicated in equation (8), whereϕ represents flow variables.

$$I = 0.16 Re^{-0.125} \quad (7)$$

$$`\frac{\partial \phi}{\partial z} = 0 \quad (8)$$

NUMERICAL METHODOLOGY

The finite volume approach [20] is used to discretize the corresponding governing equations. The simulations are carried out using ANSYSIS FLUENT-15. The unsteady

explicit module of Vof model is used with transient simulation [20]. Pressure based solver is applied. For time discretization, the first order implicit is selected while the second order upwind scheme is selected for momentum, turbulent kinetic energy and turbulent dissipation rate equations, for convergence criteria [20]. For accurate interface prediction, the Geo-Reconstruction algorithm [20] is used for volume of fluid equation. Further, variable time step is adopted to maintain 0.25 courant number value for accurate interface tracking [20]. For pressure velocity coupling, the semi-implicit pressure linked equations (SIMPLE) algorithm is used. The enhanced wall function [20] is selected for the near wall treatment. The maximum allowable error in the iteration process is set to $1x10^{-6}$.

RESULTS AND DISCUSSION

Model Validation

Checking validity and applicability of the proposed numerical issues is the first step towards realistic simulations. So, the current simulation results are compared with available previous data in literature. The experimental work of Lin et al. [12] is selected for this purpose, due to available and reliable measurements of flow inside the modelled atomizer. Fig.3-a. shows the gas phase volume fraction contours, at symmetry plane, of the current simulations compared with the experimental measurements of Lin et al. [12, 22]. The liquid is water and the gas is nitrogen. The liquid flow rate is 0.38 L/min at GLR=0.08%. It can depicted from Fig.3-a that the current results compare well with the experimental measurements. The effect of embracing inlet duct in the current simulation is obvious. Further, results of liquid film thickness (h) are compared with the experimental correlation developed by Lin et al. [12], for quantitative validation. The liquid film thickness in the present work is calculated according to the method developed by Esfarjani and Dolatabadi [16]. They assumed that the gas flows in the discharge passage of the atomizer as cylindrical core and is surrounded by the liquid, as the case in annular flow regime. The diameter of the gas passage is denoted D_g and the hydraulic diameter of the exit passage is D_h. Then the liquid film thickness (h) can be calculated by,

$$\mathrm{h} = \frac{1}{2}\left(D_h - D_g\right) \tag{9}$$

The diameter of the gas passage (D_g) is calculated using average value of gas phase volume fraction at atomizer outlet (α_g),

$$D_g = D_h\sqrt{\alpha_g} \tag{10}$$

The average value of the gas phase volume fraction at atomizer outlet is calculated after the flow reaches a statistically stationary state; the change in properties became periodic with simulation time. The area weighted average, over the outlet area, is used to sample the volume fraction at atomizer outlet. The sampling process is performed with solution time. The gas volume fraction is extracted each time step for total period of 0.005 sec. Then, averaging the values over the sampling period (0.005 sec.) is

performed to obtain final unique average value of gas volume fraction corresponding to the considered GLR. Fig.3-b. compares the current simulation results of the liquid film thickness with the experimental correlation of Lin et al. [12]. It is observed from the Fig.3-b that the current results close to great extent with the experimental measurements, which assure the accuracy of the proposed numerical issues considered in the current simulation.

Jatropha Biofuel and Jet-A1 Fuel Results

Simulations of the internal flow in effervescent atomizer with both jet-A1 fuel and jatropha biofuel are then performed. The volume flow rate of the two fuels is kept constant, for all test cases, at 0.38 L/min and the aerating gas is selected to be the air. The volume flow rate of the gas is varied to obtain the required GLR. The GLRs range and the corresponding flow rates and velocities for jet-A1 fuel and jatropha biofuel are given in table.2 and table.3, respectively. The upper limit of GLR (0.8%) is constrained by the compressibility effects associated with high velocities. The simulations are performed with variable time steps ranging from 2×10^{-6} sec to 1×10^{-9} sec. The variable time step is selected to maintain 0.25 Courant number, satisfying stability criteria and to obtain accurate interface tracking [20].

Before simulating the internal two-phase flow at different GLRs, the atomizer was tested under pure liquid operation, i.e. GLR = 0 %, for both fuels. The volume flow rate of the fuel in both cases is 0.38 L/min. The axial velocity contours at the symmetry plane, for both fuels, are shown in Fig.4. The results show recirculation zone behind the aerating tube tip for both fuels, as shown in Fig.4. It can be noticed from the figure that the recirculation zone downstream the aerating tube is shorter in case of jatropha biofuel due to the high viscosity. The wake region behind aerating tube, corresponding to recirculation, can also be noticed. Further, the liquid is accelerated in the discharge passage for both fuels due to reduction in flow area. However, while the Jatropha biofuel flows in the discharge passage, the flow is further decelerated near the walls due to the high viscosity of the biofuel. The near-wall deceleration leads to higher velocity toward center line to preserve the continuity of the flow.

Following, the gas is injected into the mixing chamber, filled with pure fuel as initial condition. At low GLR of 0.08%, the gas will penetrate into the recirculation zone, where low liquid velocity and pressure exist. Due to the low relative shear in this zone, the surface tension dominates over drag and the gas flows as continuous jet in the mixing chamber [15]. In the discharge passage inlet, the intact gas bulk will disintegrate and breaks up due to the high shear. The liquid velocity is increased due to area reduction and the drag force overcomes the surface tension; this leads to shattering the gas jet into gas slugs. These gas slugs are further elongated through their flow in the discharge passage, see Fig.5. This elongation is due to the reduction in pressure and shear accompanying high velocity [9,12, 15]. In case of jatropha biofuel, the gas slugs are larger due to the high surface tension. Further, the gas slugs become longer in the discharge passage than those of Jet-A1 fuel, due to the high shear related to high biofuel viscosity, see Fig. 5. This slug flow nature is predict to produce intermittent spray [12]. Fig.6. shows gas volume fraction in the discharge passage at two different simulation times, to indicate the effect of slug flow. Fig.7. shows the gas volume fraction contours at several planes upstream the discharge outlet in addition to the atomizer

outlet plane. These planes are taken at distances 0, 3, 6, 9, 12, 15 mms upstream and measured from the exit plane. It can be inferred from Fig.7. that the gas slugs are surrounded by liquid during their flow in discharge passage. The liquid surrounding the gas slugs is accelerated by viscous effect and reduction in available flow area. The accelerated liquid enhances the shear between the two phases and elongates the gas slugs further. It can be depicted from Fig.7. that there is no appreciable mixing between the two phase at this low aeration level. Further, mixture momentum is still centered in the core region, due to the higher gas velocity.

Further increase in GLR to 0.3% leads to an increase of the gas energy and velocity entering the mixing chamber. Fig.8. shows the gas volume fraction inside the atomizer at GLR=0.3%. Comparing the flow structure at GLR = 0.3% for both jatropha biofuel and jet-A1 fuel, it is found that at this aeration level, the effect of high surface tension dominates in case of jatropha biofuel. Further, the gas in the mixing chamber flow as smooth jet with narrow width in case of jatropha biofuel. On the other hand, the gas flows as large plugs disturbing the liquid flow in case of jet-A1 fuel, that the gas experiences less liquid resistance to expand due to the lower surface tension of jet-A1. In the discharge passage, this effect is slightly terminated as the higher surface tension results in larger gas slugs in case of jatropha biofuel. The flow structure in the discharge passage is identified as gas slugs, which are further coalescence to form annular flow, for both fuels.

At GLR=0.5%, the aeration level is increased. The gas flow has significant energy to disperse into the liquid stream and the effect of the higher surface tension of jatropha biofuel is vanished. Fig.9. presents the gas phase volume fraction inside the atomizer at GLR of 0.5% for both fuels. One can notice from Fig. 9 that the gas flows in the mixing chamber as large lumps. These gas lumps have enough energy to disturb the liquid stream and pushing the liquid toward the mixing chamber walls. The gas occupies significant portion in the mixing chamber. Also, it is obvious that the gas dispersion into the liquid is increased at this aeration level.

Towards the inlet of discharge passage, the gas phase is evolved and the gas lump breaks up into larger gas slugs. These gas slugs are further coalescence in their way to the discharge passage outlet to form annular flow regime and continuous gas stream is formed near the atomizer outlet, as shown in Fig.9. Mixing between the two phases is augmented due to the high gas velocity, that the gas reaches the atomizer walls and the liquid is squeezed toward the atomizer walls and thin liquid film is noticed, see Fig.9. In comparison with Jet-A1 results at GLR = 0.5%, the effect of jatropha biofuel surface tension is slightly inhibited at this aeration level. Large lump of gas is noticed for both fuels. In the discharge passage, the effect of higher liquid viscosity of biofuel is obvious, the higher viscosity shatters the gas continuous flow and higher shear is experienced by the gas. Further, the mixing between gas and liquid is augmented for both fuels at this aeration level (0.5%). The effect of the vortex shedding phenomenon on gas flow is significantly obvious at this aeration level. As the gas occupies large portion in the mixing chamber, the liquid velocity is increased, which increase the relative velocity and shear at the interface resulting in a wavy interface. Fig.10 shows the evolution of the vortex shedding phenomenon with simulation time for jet-A1 fuel at GLR=0.5%. The wavy gas-liquid interface can be identified from the figure.

Further increase in GLR to 0.8%, increases the potential of the gas to disperse into the liquid. Instead of gas lumps generated at lower GLRs, the gas occupies the majority of the mixing chamber, due to the increased gas quantity. Fig.11. presents the evolution of the gas flow inside the atomizer at GLR = 0.8% for both fuels. The large gas quantity existed in the mixing chamber pushes and squeezes the liquid towards the mixing chamber walls, thereby the gas flow disturbs the liquid stream. The available area for liquid flow is significantly decreased, which increases the liquid velocity, to preserve continuity of flow. This causes the two phases to exhibit excessive shear at the interface. It is observed that mixing between the phases starts in the mixing chamber.

In the discharge passage, a conflict on land arises between the large amount of gas and the liquid flow. That is finally settled by the gas due to the higher specific volume of the gas, forcing the liquid to squeeze in thin film attached to the atomizer walls. Finally the dominant gas flows as annular flow surrounded by liquid film. So, a continuous gas stream in the middle of the passage can be identified for both fuels at GLR=0.8%. The annular flow nature is identified for both the two fuel, jet-A1 and Jatropha biofuel. Fig.12. indicates the gas volume fraction contours upstream and atomizer outlet for jatropha biofuel. It is noticeable that the gas flow is surrounded by thin liquid film attached to the atomizer wall. Fig.12. also shows that majority of flow area is occupied by the gas, the gas reaches the atomizer walls, due to the high turbulence. As a result of high relative velocity, the gas is exposed to excessive shear. Significant mixing between the two phases is noticed at this aeration level. Separated liquid droplets and ligaments in gas and gas bubbles embedded in liquid can be distinguished, as shown in Fig.13., wavy interface can be identified due to high relative velocity and excessive shear. Majority of the flow area is occupied by gas at high velocity. So mixture momentum is no longer centred in the core region as the case at low GLRs. The effect of the higher biofuel viscosity is inhibited at this aeration level (0.8%) due to the larger gas quantity, which squeeze the liquid in thin film attached to the atomizer walls and pure gas flow occurred in the core region.

CONCLUSIONS

In the current study, three dimension simulations of internal two phase flow inside effervescent atomizer were performed to investigate the effect of jatropha biofuel viscosity on the flow. The volume of fluid interface tracking model was applied. For turbulence modelling, the realizable k-ε model was used. The results was fist validated with previous data available in the literature and good agreement was obtained. Further, the results of jatropha biofuel were compared with those of jet-A1 commercial aviation fuel. The current results assured that the gas to liquid mass ratio (GLR) is one of the most contributory factors affecting the flow inside the atomizer. At low GLR of 0.08%, slug flow was identified. The higher viscosity of biofuel leaded to large elongated gas slugs at this GLR. The effect of biofuel viscosity was still obvious with increasing GLR to 0.3%. The gas still has not enough energy to disperse into the liquid in case of jatropha biofuel, while the gas dispersion into the liquid was enhanced in case of jet-A1 fuel at the same aeration level of 0.3%. The flow evolved to annular flow with further increase in GLR. The effect of jatropha biofuel higher viscosity is inhibited at GLR of 0.8%. Further increase in GLR is predicted to vanish the effect of the higher biofuel viscosity on internal flow. However, these relatively high GLRs are not comparable with the GLRs ratios used with other internal mixing twin fluid atomizers,

which can reach to 50% [7]. Further, the current results revealed the superiority of effervescent atomizer on handling jatropha biofuel in terms of internal flow. Finally, simulation of the external produced spray and actual field test are the final destination towards replacement of commercial aviation jet-A1 fossil fuel with jatropha biofuel as a renewable and sustainable alternative.

REFERENCES

[1] Chevron Corporation, “Aviation Fuels Technical Review”, Annual report (2006).
[2] A. H. Lefebvre and R. B. Dilip., "Gas Turbine Combustion Alternative Fuel and Emissions", third edition, CRC press (2010).
[3] S. Baroutian, M. K. Aroua, A. A. Abdul Raman, A. Shafie, “Blended aviation biofuel from esterified Jatropha curcas and waste vegetable oils”, JTICE, Vol. 44 pp.911-916 (2013).
[4] http://www.theguardian.com/environment/2008/dec/30/biofuel-test-plane.
[5] http://www.greenaironline.com/news.php?viewStory=1110.
[6] http://www.theengineer.co.uk/first-jatropha-based-biofuel-flight-ready-for-take-off/
[7] A. H. Lefebvre, "Atomization and Spray", Hemisphere, N.Y., (1989).
[8] A. H. Lefebvre, “A Novel Method of Atomization with Potential Gas Turbine Application”, Indian Defense Sci., Vol. 38, pp. 353-62 (1988).
[9] D. Sen, M. A. Balzan, D. S. Nobes and B. A. Fleck, “Bubble formation and flow instability in an effervescent atomizer”, J. Vis, Vol. 17, pp. 113-122 (2014).
[10] H. E. Buckner and P. E. Sojka, “Effervescent Atomization of High Viscosity Fluids. Part 1: Newtonian Liquids”, Atomization and Sprays, Vol. 1, pp. 239-52 (1991).
[11] Sovani S.D., Sojka P. E. and Lefebvre A. H. “Effervescent Atomization”, Prog. Energy Combust. Sci., Vol. 27, pp. 483-521 (2001).
[12] K. C. Lin, P. J. Kennedy and T. A. Jackson, “Structures of Internal Flow and the Corresponding Spray for Aerated-Liquid Injectors”, AIAA, NO 3569, PP. 1-12 (2001).
[13] M. H. Jobehdar, "Experimental Study of Two-Phase Flow in a Liquid Cross-Flow and an Effervescent Atomizer", Master Thesis, Western University (2014).
[14] M. Loscher, S. Florian and M. Dieter, “Flow Field and Phase Distribution Inside Effervescent Atomizers”, ILASS-Europe (2003).
[15] D. Law, T. Shepard and I. Wardi, “A Combined Numerical and Experimental Study of Air Bubble Dynamics in Converging Section of Effervescent atomizer”, AJK Fluids Conference (2015).
[16] S. A. Esfarjani, and A. Dolatabadi, “A 3D Simulation of Two-Phase Flow in an Effervescent Atomizer for Suspension Plasma Spray”, Surf. Coatings Tech., Vol.203, PP. 2074–2080 (2009).
[17] K. Mehmood and J. Masud, “Analysis of Two-Phase Flow in an Effervescent Atomizer Using Volume of Fluid Method”, AIAA 50th Meeting, Tennessee, No. 0312 (2012).
[18] D. Law, T. Shepard and P. Strykowski “Numerical Simulations of Near-Nozzle Exit Characteristics for an Effervescent Atomizer at Low Gas to liquid Mass Flow Ratio”, FEDSM Conference (2014).

[19] Hirts C. W. and Nicholas B. D., "Volume of Fluid (VOF) Method for the Dynamic of Free Boundaries", J. of Computational Physics, Vol. 39, PP. 201-255 (1981).
[20] FLUENT, Computational Fluid Dynamics Software Package User Guide, Ver. 6.3, Fluent Inc, Lebanon, NH (2006).
[21] J. U. Brackbill, D. B. Kothe and C. Zemach, "A Continmium Method for Modelling Surface Tension", J. of computational physics, Vol.100, PP. 335-354 (1992).
[22] A. Tian, "Numerical Simulation of Transient Two-Phase Flow within Aerated-Liquid Injectors", AIAA, 4266 (2003).

Table 1. Comparison between jatropha biofuel and jet-A1 properties [1, 3].

properties / fuel type	viscosity (pa.s) $\times 10^{-3}$	Surface tension (N/m) $\times 10^{-3}$	Density (kg/m^3)	Heating value (Mj/kg)
jatropha biofuel	4.4556	30.5	874	38-41
jet-A1 aviation fuel	1.0254	23.8	815	44-46

Table 2. Jet-A1 and air velocities and mass flow rates at different GLRs.

GLR (%)	jet-A1 mass flow rate (kg/sec)	jet-A1 velocity (m/sec)	air mass flow rate (kg/sec)	air velocity (m/sec)
0.08	5.19 E-3	0.58	4.13 E-6	7.43
0.15	5.19 E-3	0.58	7.74E-6	13.93
0.30	5.19 E-3	0.58	1.55E-5	27.86
0.50	5.19 E-3	0.58	2.58E-5	46.44
0.80	5.19 E-3	0.58	4.13E-5	74.31

Table 3. Jatropha and air velocities and mass flow rates at different GLRs.

GLR (%)	Jatropha mass flow rate (kg/sec)	jatropha velocity (m/sec)	air mass flow rate (kg/sec)	air velocity (m/sec)
0.08	5.53 E-3	0.58	4.43 E-6	7.97
0.15	5.53 E-3	0.58	8.30E-6	14.95
0.30	5.53 E-3	0.58	1.66E-5	29.89
0.50	5.53 E-3	0.58	2.77E-5	49.82
0.80	5.53 E-3	0.58	4.43E-5	79.69

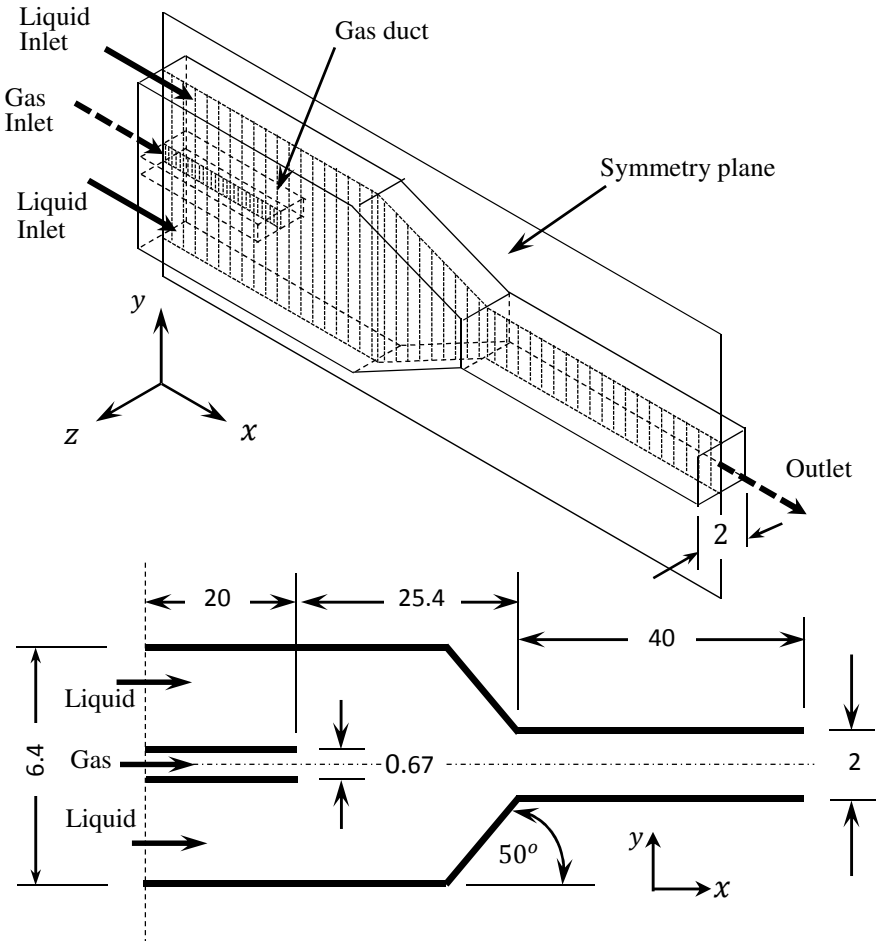

Fig.1. Details of effervescent atomizer model used in present work (Dimensions are in mm).

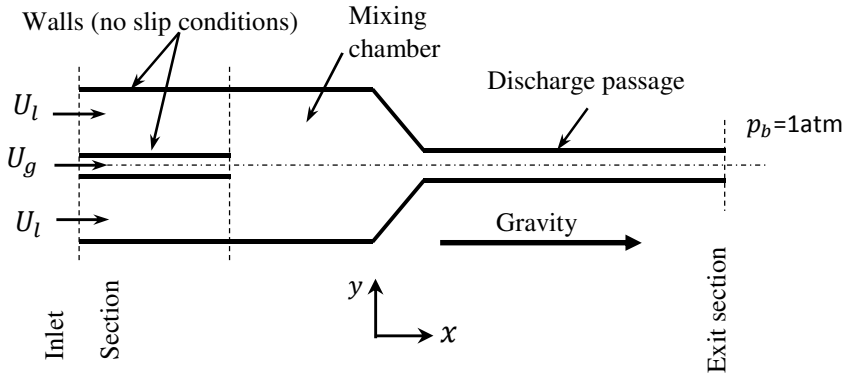

Fig.2. Boundary conditions encountered.

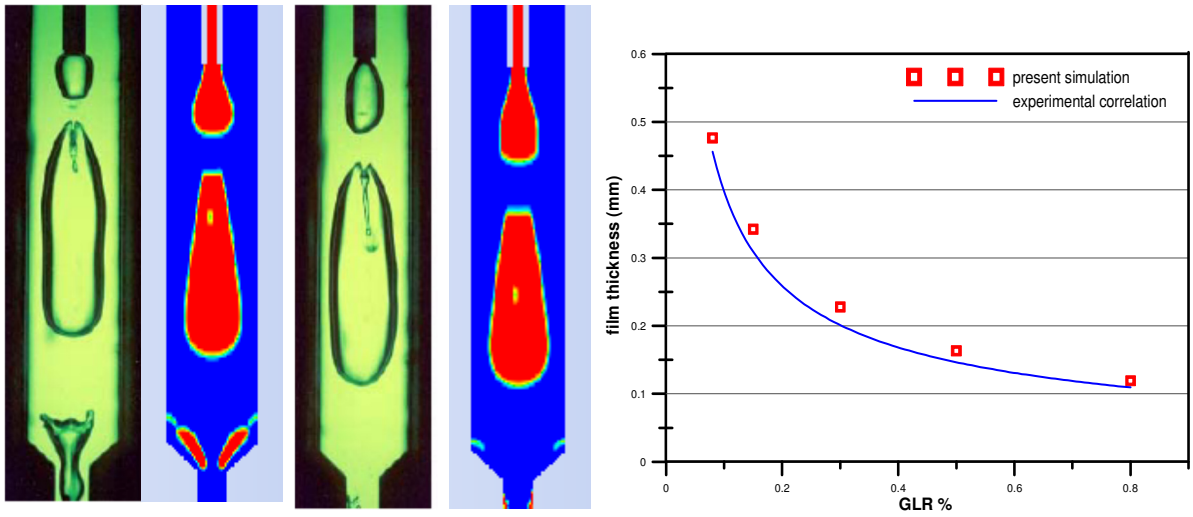

time = 0.0168 sec. time = 0.0328 sec

a) Internal flow structure

b) Liquid film thickness

Fig. 3. Comparison between current simulation results and the experimental measurements of Lin et al. [12].

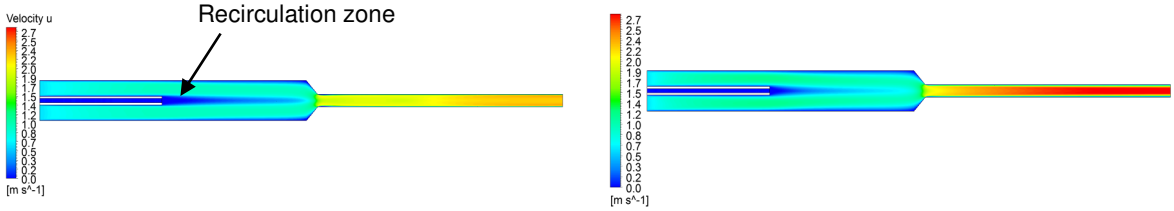

a) Jet-A1 fuel

b) Jatropha biofuel

Fig. 4. Axial velocity contours at symmetry plane.

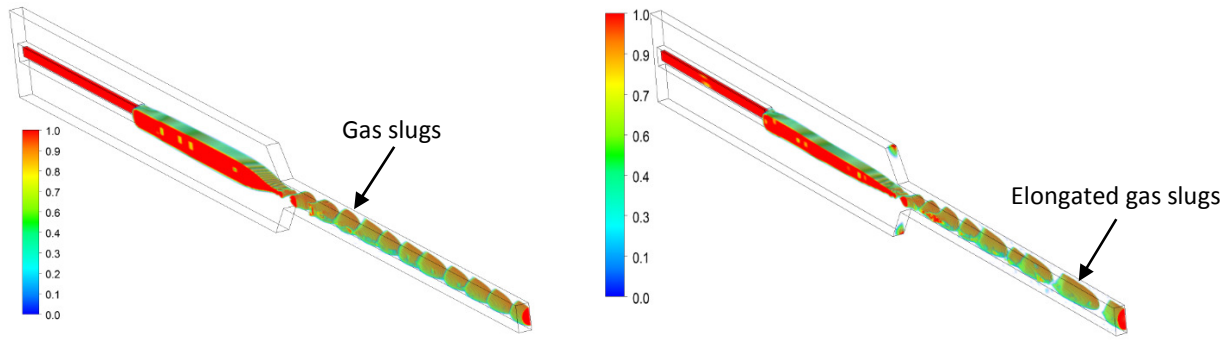

a) Jet-A1 fuel time= 0.0644 sec.

b) Jatropha biofuel time =0.0565 sec.

Fig. 5. Gas phase volume fraction at GLR=0.08%.

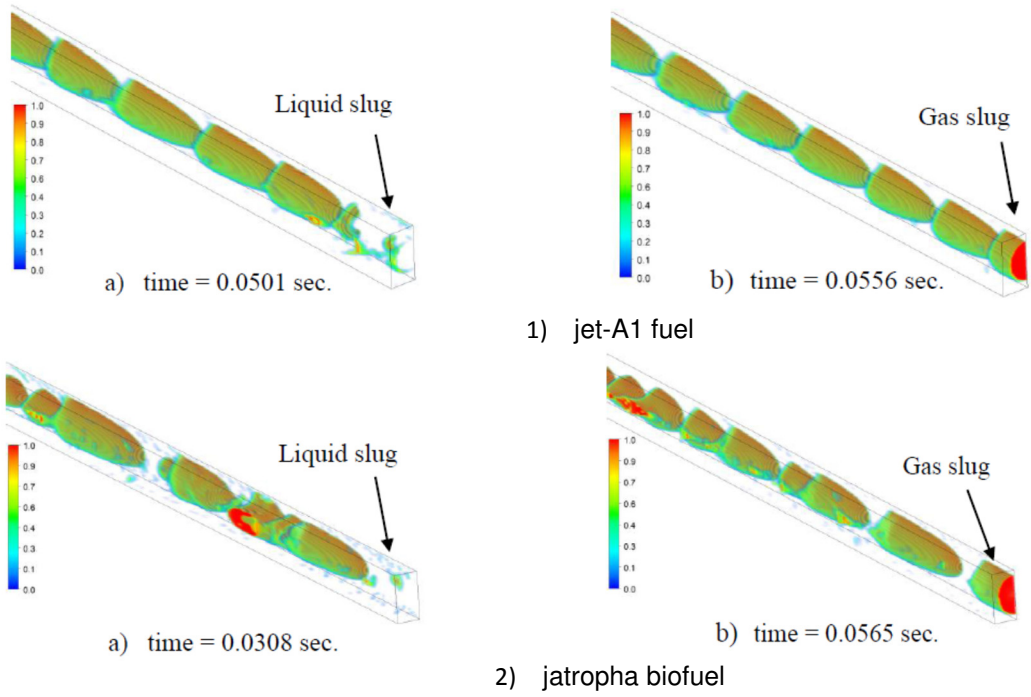

Fig. 6. Gas phase volume fraction through discharge passage at GLR=0.08%.

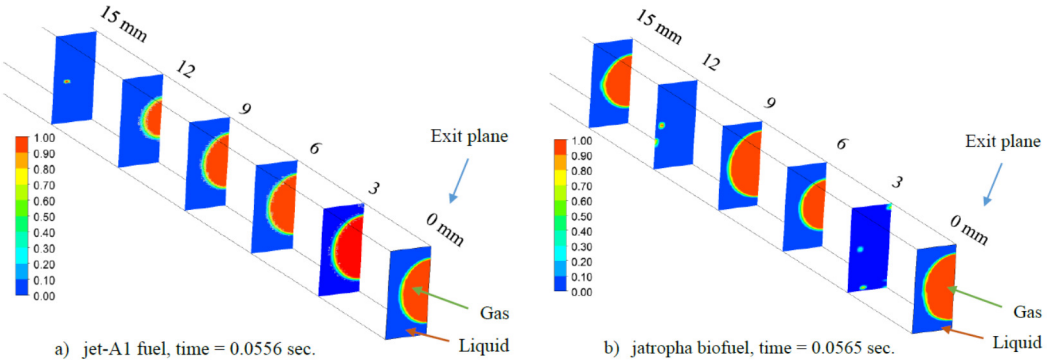

1) jet-A1 fuel time= 0.0644 sec. 2) jatropha biofuel time =0.0565 sec.

Fig. 7. Gas phase volume fraction at GLR=0.08%.

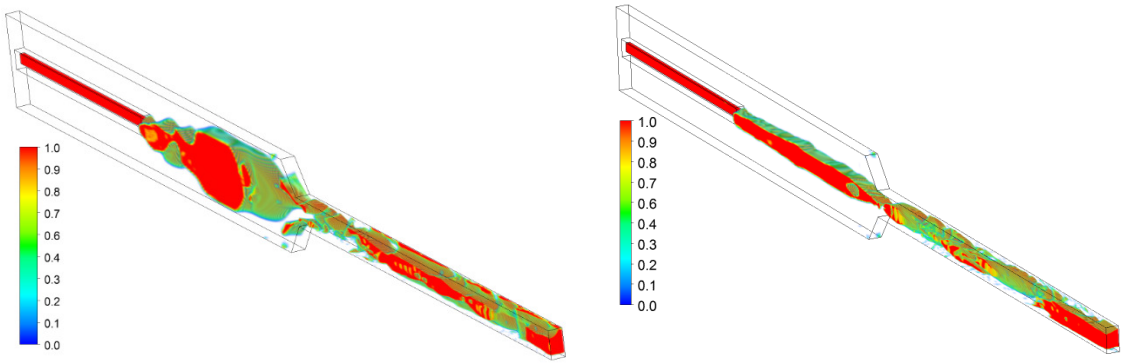

a) Jet-A1 fuel time= 0.0644 sec. b) Jatropha biofuel time =0.0565 sec.

Fig. 8. Gas phase volume fraction at GLR=0.3%.

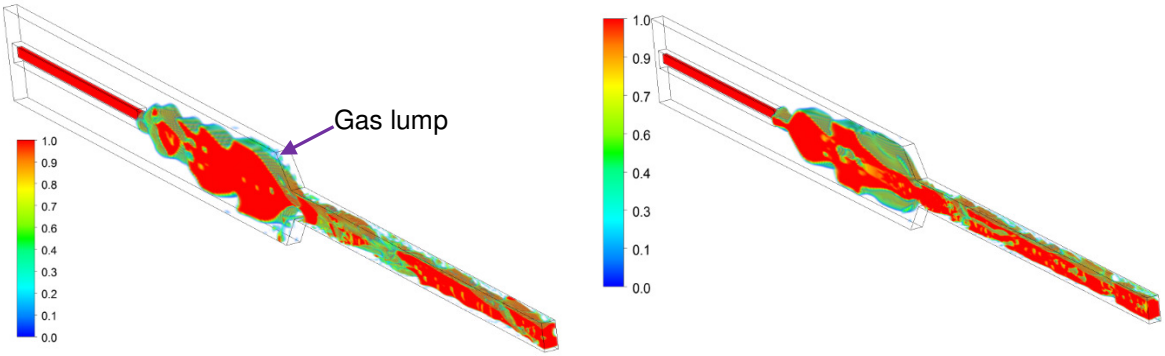

a) Jet-A1 fuel time= 0.0307 sec. b) Jatropha biofuel time =0.0241 sec.

Fig. 9. Gas phase volume fraction at GLR=0.5%.

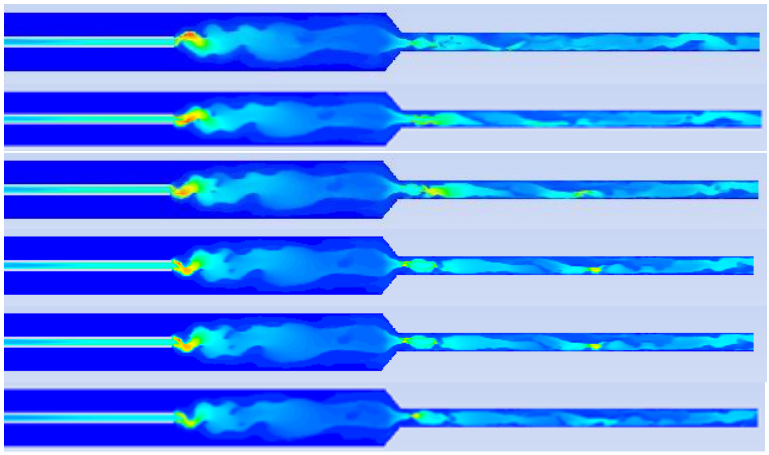

Fig. 10. Vortex shedding phenomenon for simulation period of 0.002 sec. at GLR = 0.5%.

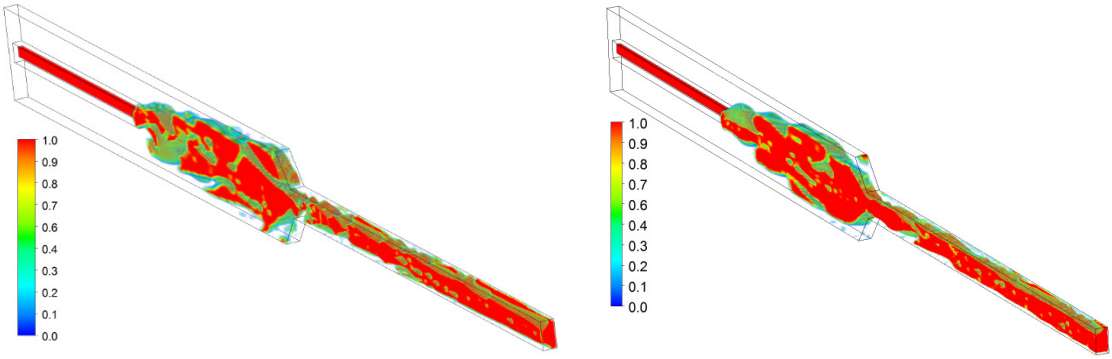

a) Jet-A1 fuel time= 0.0193 sec. b) Jatropha biofuel time =0.0243 sec.

Fig. 11. Gas phase volume fraction at GLR=0.8%.

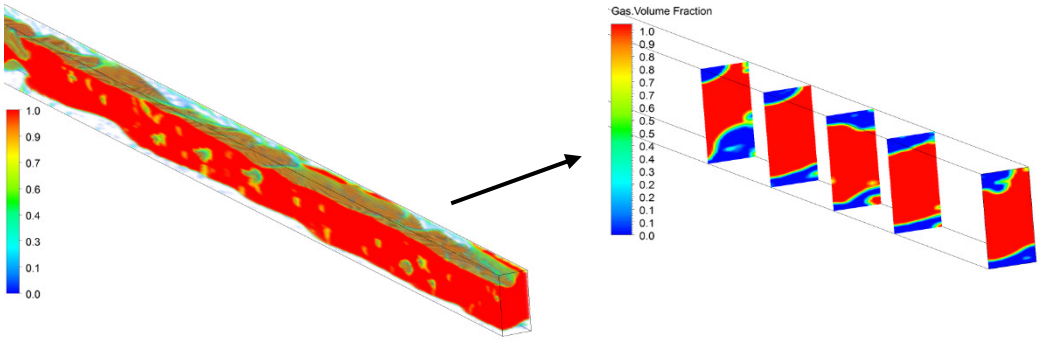

Jatropha biofuel time= 0.0243 sec.

Fig. 12. Gas phase volume fraction in discharge passage at GLR=0.8%.

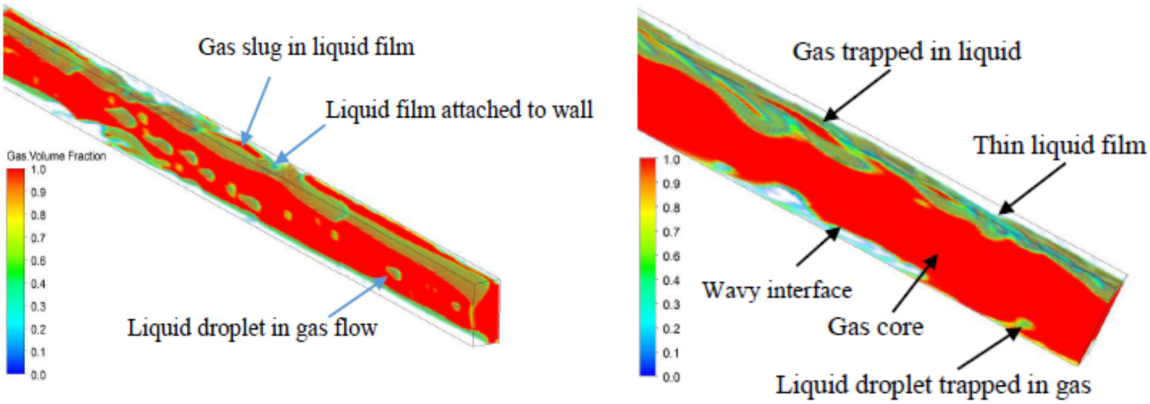

a) Jet-A1 fuel time= 0.0193 sec. b) Jatropha biofuel time =0.0194 sec.

Fig. 13. Gas phase volume fraction in discharge passage at GLR=0.8%.